NANO LETTERS

2007
Vol. 7, No. 12
3753−3758

Micrometer and Nanometer Scale Photopatterning of Self-Assembled Monolayers of Phosphonic Acids on Aluminum Oxide

Shuqing Sun and Graham J. Leggett*

Department of Chemistry, University of Sheffield, Brook Hill, Sheffield S3 7HF, U.K.

Received August 28, 2007; Revised Manuscript Received October 16, 2007

ABSTRACT

Self-assembled monolayers of alkylphosphonic acids (APA) have been patterned at the micrometer and nanometer scale by photochemical methods. Exposure of APA monolayers to light with a wavelength of 244 nm leads to scission of the C–P bond and desorption of the alkyl chain from the surface. Immersion of the specimen in a solution of a second APA leads to adsorption at the surface in the exposed regions. Immersion in a solution of hydroxide ions leads to etching of the exposed regions of the aluminum film. UV exposure appears to anneal the aluminum oxide film, conferring increased resistance to etching at high exposures and a switching the function of the monolayer from a positive to a negative tone resist. At intermediate exposures, nanoscale trenches form at the perimeters of exposed regions. Near-field exposure of the phosphonic acid structures, using a UV laser coupled to a scanning near-field optical microscope, yields well-defined nanostructured features following development of the pattern in aqueous base, exemplified by the fabrication of 100 nm wide trenches.

There has been a great deal of interest in the fabrication of molecular nanopatterns for applications ranging from molecular electronics through sensing to applications in biological diagnostics. Much work to date has focused on self-assembled monolayers of alkanethiols adsorbed onto gold surfaces. While these possess exceptional order and chemical stability and may be patterned conveniently by a range of methods including dip-pen nanolithography,[1−5] near-field photolithographic methods,[6−11] scanning tunneling techniques,[12] electron beam lithography, and nanoshaving/nanografting,[13−18] the propensity of gold to quench fluorescence and the limited ambient stability[19,20] of alkanethiol systems mean that alternative systems may be attractive. Siloxane monolayers exhibit very high ambient stability, and Sagiv has successfully patterned them using local oxidation techniques[21,22] in which a conductive atomic force microscopy (AFM) tip is brought close to a surface under an applied potential difference. In this laboratory, we have utilized scanning near-field photolithography (SNP) to modify silane monolayers containing photoactive terminal groups.[8] However, siloxane monolayers lack the high degree of order associated with self-assembled monolayers (SAMs) of alkanethiols on gold.

Alkylphosphonic acids self-assemble onto oxide surfaces to form dense, highly ordered monolayers.[23−26] The mechanism of attachment to the surface depends upon the substrate.[27] On surfaces primed with cations, a strong electrostatic interaction forms following deprotonation of the head group. On other surfaces, such as titania, there is evidence that dissociation of the hydroxyl functional groups may be incomplete, yielding a weaker interaction. On aluminum, a condensation reaction is thought to occur between the deprotonated acid and hydroxyl groups at the oxide surface, leading to the formation of phosphonate functionalities at the surface that exhibit a symmetrical tridentate structure.[28] Numbers of gauche defects are very low, as small as 1−4%.[29] Mallouk and co-workers[30] determined that the head group separation is 0.48 nm for phosphonate salts adsorbed on small divalent metal ions, similar to the 0.499 nm widely reported for alkanethiols adsorbed on Au. Moreover, Byrd et al. reported a contact angle of 110° and a tilt angle of ca. 22° for octadecylphosphonic acid monolayers adsorbed on a zirconated Langmuir Blodgett template,[31] similar to the values reported for monolayers of alkanethiols on gold and silver. Recent work in the authors' laboratory using friction force microscopy in conjunction with polarization-modulation reflection−absorption infrared spectroscopy)[32] is consistent with these hypotheses and additionally suggests that phosphonic acid monolayers exhibit exceptional stability to ambient exposure. For example, the coefficient of friction of decylphosphonic acid monolayers on aluminum oxide is unchanged after 700 h in contrast to monolayers of decanethiol on gold, which exhibit a significant change in their

* Corresponding author. E-mail: Graham.Leggett@shef.ac.uk.

10.1021/nl072181+ CCC: $37.00
Published on Web 11/10/2007

coefficient of friction (indicative of extensive oxidative degradation) after only 24 h exposure.[20]

Besides the expected benefits of reduced fluorescence quenching compared to gold surfaces, phosphonic acid monolayers have potential applications in many other areas of nanoscience. For example, aluminum is an important material in electronic device fabrication, and well-defined oxide films may be grown on aluminum surfaces and used as gate dielectrics in transistors. However, despite the potential importance of oxide surfaces in nanoscience, comparatively little attention has been directed toward the patterning of monolayers on oxide substrates, and phosphonic acid monolayers remain neglected despite their many advantages. In this study, we report that photopatterning of phosphonic acid monolayers may be accomplished readily at 244 nm to yield patterned molecular assemblies with dimensions from the micrometer to the nanometer scale. Patterned phosphonic acid monolayers may be used as resists for the etching of structures into aluminum substrates.

Monolayers of octadecyl phosphonic acid molecules were prepared by immersion of aluminum-coated glass microscope slides in solutions of the adsorbate in degassed ethanol for at least 12 h. A 10 nm sample of Cr was first deposited onto the substrates, and aluminum was then deposited at a rate of less than 1 nm s^{-1} to a thickness of 100 nm. SAMs were characterized, following rinsing in ethanol and drying, by contact angle measurement using a Rame−Hart model 100-00 contact angle goniometer and a drop size of about 2 μL. Contact angles were in the range 105−115°. X-ray photoelectron spectroscopy (XPS) was also carried out using a Kratos Axis Ultra spectrometer (Kratos Analytical, Manchester, UK), equipped with a monochromatized Al Kα X-ray source. The resulting XPS spectra were analyzed using the CasaXPS program (Casa, http://www.casaxps.com, U.K.).

A Coherent Innova 300C FreD argon ion laser (Coherent (U.K.) Ltd, Ely, U.K.), emitting at 244 nm, was utilized to carry out SAM photooxidation. Micropatterns were generated by using a transmission electron microscopy mesh grid (Agar, Cambridge, UK) as a photomask that was brought into contact with the samples before being exposed to an expanded laser beam with the diameter of the spot size of either ca. 1.5 cm for XPS measurements or 0.7 cm for micropatterning. Except where otherwise stated, the laser power was 100 mW. Micropatterned SAMs containing amine-functionalized regions separated by regions occupied by methyl-terminated phosphonic acid were prepared by dipping micropatterned samples in an aqueous solution of amino-butylphosphonic acid for 30 min. SNP was performed using ThermoMicroscopes Aurora III NSOM systems (Veeco, Cambridge, U.K.). Light from the frequency-doubled argon ion laser was coupled to the end of the fiber probe through an optical coupler. A scan speed of 1 μm s^{-1} was used. After exposure, the samples were dipped in a 0.4 M sodium hydroxide etching solution for 0.5−5 min to create three-dimensional structures in the underlying substrate.

Micropatterned and nanopatterned SAMs containing amine-functionalized regions separated by regions occupied by methyl-terminated thiols were immersed for 30 min in solutions containing 5 μL of 100 nm diameter aldehyde-coated polymer nanoparticles (Duke Scientific, Palo Alto, CA; polystyrene microspheres, 4% solids) in 0.1 M pH 6 2-(*N*-morpholino)ethanesulfonic acid buffer.

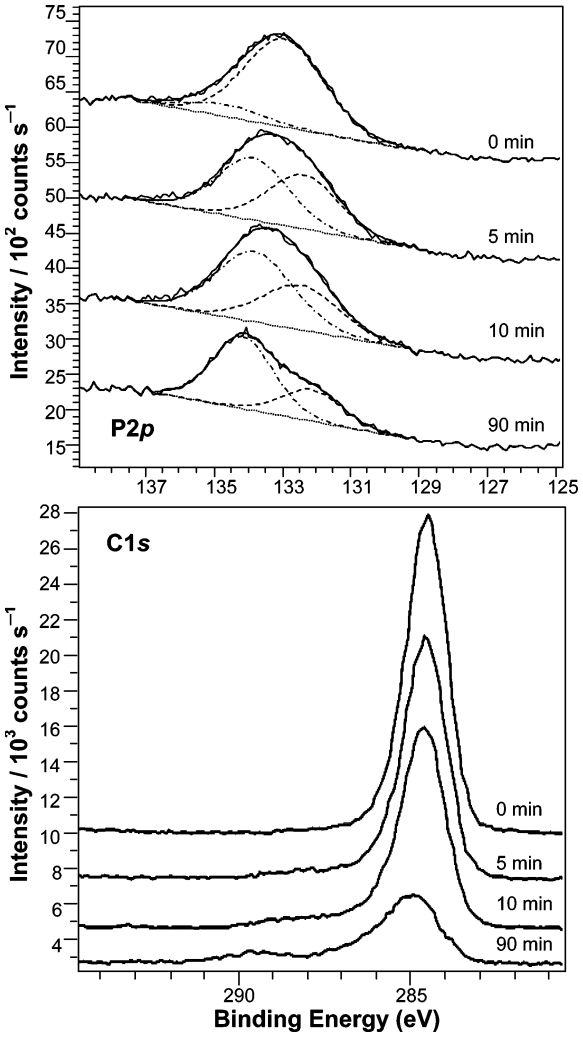

Figure 1. P2p (top) and C1s (bottom) regions of the XPS spectra of octadecyl phosphonic acid monolayers following exposure to UV light.

Phosphonic acid monolayers were exposed to UV light and characterized using XPS. Figure 1 shows the variation in the C1s and P2p regions of the XPS spectrum as a function of exposure for octadecyl phosphonic acid monolayers. The area of the P2p peak remained comparatively unchanged as a function of the UV exposure time. The spectrum was fitted with two components. For the virgin film, the low binding energy component (133.2 eV) was dominant, and the high binding energy component (135 eV) was of very small intensity. As exposure increased, the high binding energy component increased in relative intensity and was the dominant one at 90 min exposure. The presence of the high binding energy component after exposure to UV radiation may be associated with the presence of phosphorus in a higher oxidation state, possibly corresponding to a phosphate species rather than a phosphonate.

The size of the C1s peak decreased with exposure over the same time period. After 5 min, the C/Al ratio had dropped

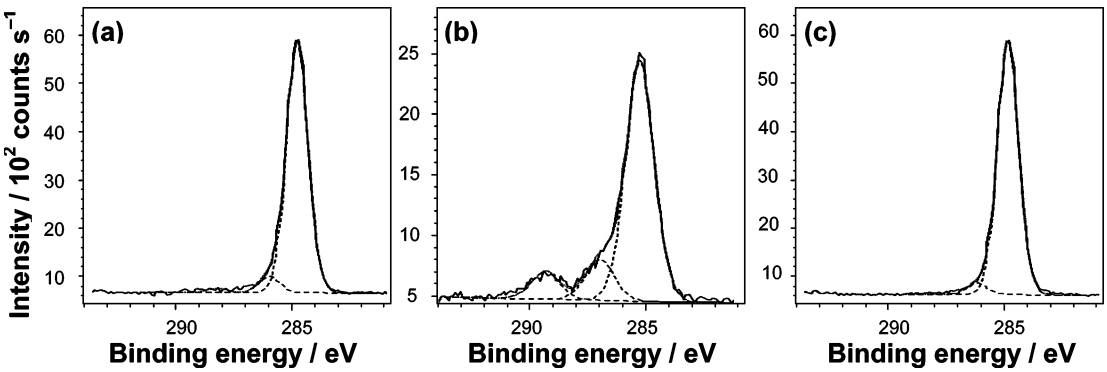

Figure 2. XPS C1s spectra of an octadecylphosphonic acid monolayer (a) before and (b) after 90 min exposure to UV irradiation and (c) following immersion of the sample in a fresh solution of the same adsorbate.

from 2.86 to 2.00 and the C/P ratio from 6.16 to 4.36, while the P/Al ratio remained unchanged at 0.46. Increasing the exposure to 10 min yielded further changes in the C/Al and C/P ratios to 1.66 and 3.8, respectively. The P/Al ratio remained virtually unchanged (0.44). However, at very long exposures, the P/Al ratio declined. At 90 min exposure, it had decreased to 0.27.

Additionally, there was a change in the shape of the C1s spectrum following UV exposure with an asymmetry developing on the high binding energy side of the main peak after short exposures, and a strong feature being observed at a chemical shift of ca. 4.4 eV after 90 min, probably corresponding to the formation of a carboxylate functionality. Figure 2b shows a deconvoluted C1s spectrum of an oxidized monolayer.

While the P/Al ratio remains at first little changed, the reduction in the C/Al ratio is best explained by the scission of the P−C bond as a result of UV exposure, leading to the desorption of the alkyl chain and/or fragments of it while the phosphorus remains at the surface. The high binding energy component of the P2p spectrum is consistent with the formation of residual phosphate species following removal of the alkyl chain. The appearance of the new feature in the C1s region at 289.4 eV may suggest that this process is accompanied by photolytic oxidation of the alkyl chain to yield species that subsequently remain coordinated to the aluminum oxide surface. However, it may additionally indicate the adsorption of carbonaceous contaminants to the high-energy surface resulting from removal of the adsorbates. This may explain why the P2p peak area remains constant for exposures up to 10 min; in fact, removal of the adsorbate alkyl chain would be expected to lead to a small increase in the P2p area because of the reduction in the thickness of the overlayer that attenuates the photoelectrons from P. The fact that the P2p signal remains constant may indicate that while the monolayer is being degraded, contaminants are being added. Such behavior would be consistent with a previous study of the rapid build-up of contamination layers on aluminum oxide films,[20] which yielded C1s spectra similar to the one shown in Figure 2b.

On exposure to a solution of a second phosphonic acid the oxidation products could be replaced. Figure 2 shows the C1s spectrum of an octadecylphosphonic acid monolayer before and after exposure to 90 min illumination with UV light. The reduction in the peak area and the appearance of strong peaks corresponding to oxycarbon species are clear. After immersion in a solution of the same adsorbate in ethanol, however, the oxidation products were displaced from the surface and the C1s spectrum of the resulting material in Figure 2c was indistinguishable from that of the fresh monolayer in Figure 2a. A small asymmetry is present in the spectra in Figure 2a and b. The origin of this is not clear. The presence of the phosphate residue at the surface appeared not to damage the integrity of the resulting monolayer; indeed, the ordering of the second monolayer, formed subsequent to C−P bond scission, seemed if anything better because monolayers formed on substrates that had previously been covered with adsorbates and then exposed to UV illumination exhibited much improved resistance to erosion by sodium hydroxide, indicative of closer packing and enhanced order.

Photopatterned phosphonic acid monolayers were formed by exposing methyl-terminated monolayers to UV light through a mask. For these experiments, the laser spot diameter was reduced from 1.5 to 0.7 cm, leading to a decrease in the area by a factor of ca. 5. The laser power remained unchanged, so the effective dose rate increased by a factor of ca. 5. The samples were then immersed in a solution of aminobutyl phosphonic acid, and the resulting pattern imaged using friction force microscopy. Figure 3 shows a friction force microscopy (FFM) image of a representative example. FFM is a powerful tool for the characterization of such patterns because different frictional responses are measured for regions of different polarity. In the present case, a silicon nitride cantilever was used where the outer surface consists of a thin layer of silicon dioxide. This polar material interacted strongly with polar regions of the sample, yielding enhanced adhesion compared to the nonpolar regions. Consequently, the rate of energy dissipation was greater as the tip slid across the amine-terminated regions than when it interacted with the methyl-terminated regions, leading to a larger friction force and brighter contrast. The resulting patterns exhibited clear contrast with straight edges and faithful reproduction of the dimensions of the features in the mask.

To further test that molecular patterns had formed correctly, functionalized nanoparticles were used to derivatize

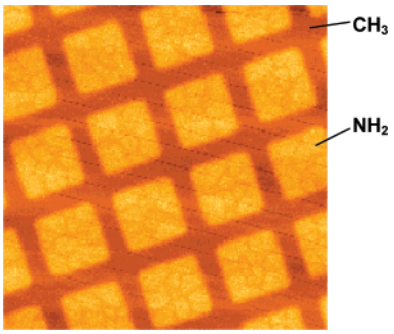

Figure 3. 100 × 100 μm^2 friction force microscopy image of a patterned monolayer formed by exposure of a monolayer of octadecyl phosphonic acid to UV light for 5 min at a power of 100 mW and subsequent emersion of the sample in a solution of aminobutyl phosphonic acid in water.

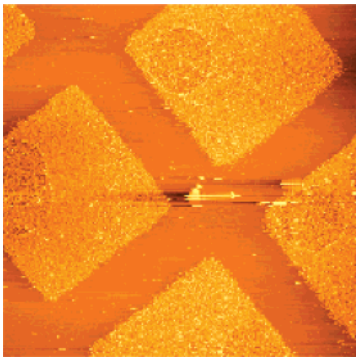

Figure 4. 100 × 100 μm^2 AFM topographical image showing aldehyde-functionalized polymer nanoparticles attached to patterns of phosphonic acid adsorbates with methyl (bars) and amine (squares) terminal groups. Image size: 100 × 100 μm^2.

amine-terminated regions. A methyl-terminated monolayer was first formed then exposed to UV light through a mask to selectively remove adsorbates. The sample was then immersed in a solution of aminobutyl phosphonic acid to derivatize the exposed areas and then in a solution of aldehyde-functionalized polymer nanoparticles. The aldehyde groups can react with amines to form imine linkages, thus attaching them to the amine-terminated regions but not the methyl-terminated ones. Figure 4 shows a topographical AFM image of a sample prepared in this way. There is clear height contrast between the exposed areas (which appear raised) and the masked ones, and the nanoparticles may be resolved, densely covering the square regions. It should be noted that XPS spectra of samples following immersion in a solution of aminobutylphosphonic acid yielded small N1s peaks. This is attributed to the competition between adsorption and etching that occurs when the aluminum oxide is exposed to a solution of a phosphonic acid in water; water is known to destabilize phosphonic acids adsorbed on oxide surfaces. This procedure is likely only to yield low densities of amine groups at the oxide surface therefore, although Figure 4 indicates that the density is high enough for dense attachment of nanoparticles. Future work should thus focus on the use of adsorbates that are soluble in nonaqueous solvents in the second step of the process.

Aluminum and its oxide are susceptible to dissolution in sodium hydroxide. To determine the effectiveness of photopatterned phosphonic acid monolayers as resists for the etching of structures into aluminum films, samples were exposed to a 0.4 Mol dm^{-3} aqueous solution of sodium hydroxide following exposure to UV light through a mask. It was found that the nature of the features that were formed depended on the time of exposure to UV light, effecting significant control over the morphology of the etched film. For samples exposed to UV light for between 0.5 and 2 min, the resulting morphology was similar to that shown in Figure 5a (which shows a sample exposed for 1 min). After immersion of the sample in the sodium hydroxide solution, the exposed regions (the squares) are seen to have been eroded. The height difference between the masked and exposed areas in Figure 5a is 65 nm, commensurate with removal of the passive oxide film and also etching of the underlying Al exposed by removal of the oxide.

As the exposure time increased, the height difference between the masked and exposed areas following etching declined (exposures between 2 and 15 min). Eventually exposures were reached at which little difference was seen between the masked and the exposed areas (Figure 5b). The predominant topographical features followed the perimeters of the masked areas, yielding narrow troughs 1500−1800 nm wide that completely encircled the exposed areas. As the exposure increased still further (from 15 min upward), an inversion of contrast was observed with the exposed areas now being higher than the masked areas after etching (by ca. 40 nm). In this latter case, the exposed regions of the sample remained apparently unaltered, and the masked regions, that is, those that are protected by phosphonic acid adsorbates, appeared to have been eroded. It should be noted that the time required to develop the pattern in Figure 5c using sodium hydroxide was longer than that required for development of the low-exposure pattern (Figure 5a).

Given that phosphonic acid monolayers are not very stable in aqueous conditions, it is not surprising that the masked areas are eroded at longer etching times: the etchant will first erode the adsorbate layer and then the underlying oxide. What is much more surprising is that after long UV exposures, significantly greater than required for complete removal of the adsorbate layer, the oxide apparently becomes resistant to the etch solution. The most likely explanation for this behavior is the modification of the aluminum oxide layer by UV light, rendering it sufficiently resistant to the action of the etchant that it remains intact over long immersion times during which the monolayer-protected regions are removed (initially, presumably through attack at defect sites). While at first sight it might be thought feasible that UV exposure causes thickening of the oxide film, conferring an improved level of protection to the exposed areas, this explanation can be discounted, because there was no evidence of a height increase in the regions exposed to UV light through the mask. Any change must involve the modification of the oxide structure, rather than simple thickening. Such a modification may explain the reduction in the P/Al ratio at 90 min exposure in Figure 1, which is a

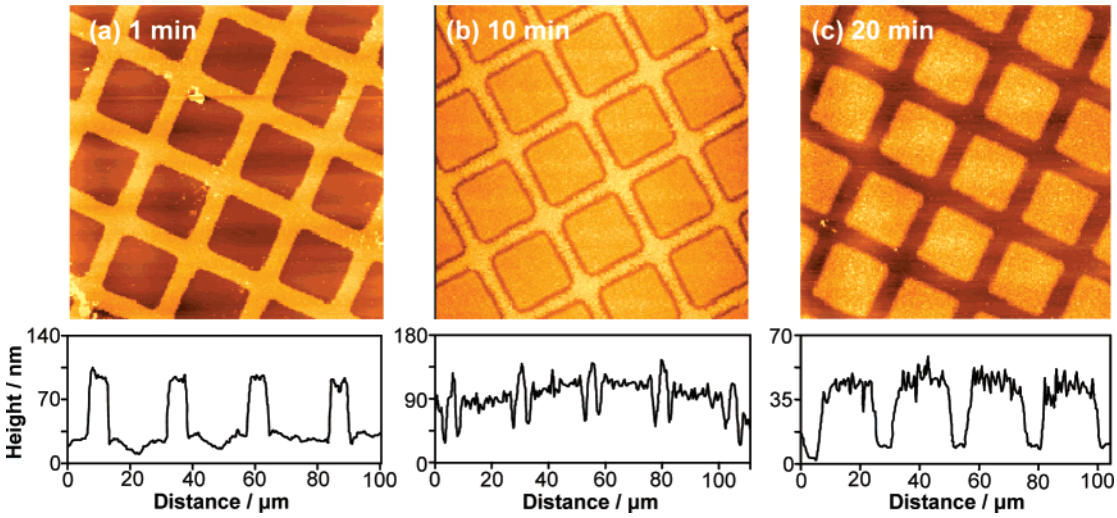

Figure 5. 100 × 100 μm^2 tapping mode AFM topographical images and representative line sections for photopatterned monolayers of octadecyl phosphonic acid on aluminum following exposure to UV light for different periods of time and immersion in an aqueous 0.4 Mol dm^{-3} solution of sodium hydroxide.

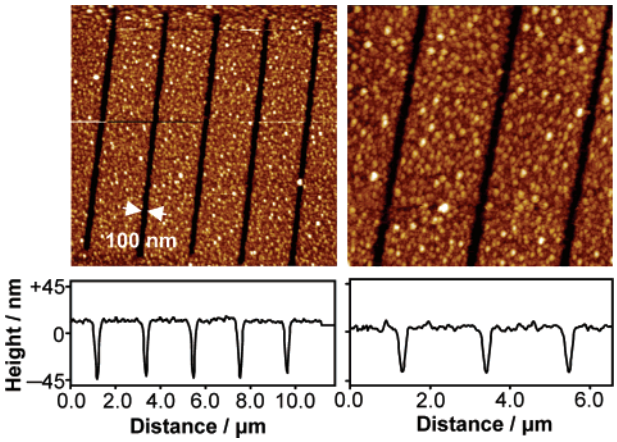

Figure 6. Tapping mode AFM images of nanostructures formed by using SNP-patterned phosphonic acid monolayers as resists for the etching of Al. Image sizes: 11 × 11 μm^2 (left) and 6 × 6 μm^2 (right). The line sections reveal that the depths of the trenches are 61 nm (left) and 41 nm (right).

similar exposure, given the five times larger area, to that used to generate the sample imaged in Figure 5c.

Nanometer scale patterns were fabricated by exposing phosphonic acid monolayers to UV light from a scanning near-field optical microscope (SNOM) (SNP). At a power of 10 mW and a writing rate of 1 $\mu m\ s^{-1}$, it was possible to fabricate nanopatterns that could be used as resists for nanometer etching of the Al film. Figure 6 shows illustrative results. A series of lines have been written using the SNOM, and the sample has been immersed in a 0.4 Mol dm^{-3} solution of sodium hydroxide for ~0.5 min. The sodium hydroxide etched the metal exposed following UV exposure, leading to the formation of well-defined trenches ca. 100−120 nm in width. These are slightly larger than structures etched into gold films using SNP in conjunction with a ferri/ferrocyanide etch solution and approximately three times wider than structures previously reported for gold using mercaptoethylamine as the etchant. In large measure, this is probably attributable to the larger grain size of the Al film when compared with gold. It is possible to prepare gold films with smaller grain sizes, which enable narrower structures to be fabricated with good edge definition. Nevertheless, the features reported here represent a significant and useful new direction for scanning probe lithography.

In summary, these data indicate that photopatterning provides a facile route to the fabrication of patterned structures on length scales from the micrometer to the nanometer. Irradiation at 244 nm initiates C−P bond cleavage. Immersion of the substrate in a solution of a second adsorbate at the surface leads to the reformation of a monolayer. Immersion in a solution of aqueous base causes etching. When used in conjunction with near-field exposure, this approach yields structures as small as 100 nm. UV exposure modifies the structure of the aluminum oxide surface, conferring enhanced stability against aqueous bases. By controlling the exposure, it is possible to switch the function of the phosphonic acid monolayer from that of a positive to a negative tone resist. Phosphonic acid monolayers offer great promise as the basis for molecular patterning on oxide substrates.

Acknowledgment. The authors thank Research Councils U.K. (Grant EP/C523857/1) for financial support. G.J.L. thanks the Engineering and Physical Sciences research Council (EPSRC) and Royal Society of Chemistry Analytical Chemistry Trust Fund for support.

References

(1) Hong, S.; Zhu, J.; Mirkin, C. A. *Science* **1999**, *286*, 523−525.
(2) Lee, K.-B.; Park, S.-J.; Mirkin, C. A.; Smith, J. C.; Mrksich, M. *Science* **2002**, *295*, 1702−1705.
(3) Lee, K.-B.; Lim, J.-H.; Mirkin, C. A. *J. Am. Chem. Soc.* **2003**, *125*, 5588−5589.
(4) Nam, J.-M.; Lee, K.-B.; Liu, X.; Ratner, M. A.; Mirkin, C. A. *Angew. Chem., Int. Ed.* **2004**, *43*, 1246−1249.
(5) Hyun, J.; Ahn, S. J.; Lee, W. K.; Chilkoti, A.; Zauscher, S. *Nano Lett.* **2002**, *2*, 1203−1207.
(6) Sun, S.; Chong, K. S. L.; Leggett, G. J. *J. Am. Chem. Soc.* **2002**, *124*, 2414−2415.
(7) Sun, S.; Leggett, G. J. *Nano Lett.* **2004**, *4*, 1381.

(8) Sun, S.; Montague, M.; Critchley, K.; Chen, M.-S.; Dressick, W. J.; Evans, S. D.; Leggett, G. J. *Nano Lett.* **2006**, *6*, 29−33.
(9) Montague, M.; Ducker, R. E.; Chong, K. S. L.; Manning, R. J.; Rutten, F. J. M.; Davies, M. C.; Leggett, G. J. *Langmuir* **2007**, *23*, 7328−7337.
(10) Ducker, R. E.; Leggett, G. J. *J. Am. Chem. Soc.* **2006**, *128*, 392−393.
(11) Leggett, G. J. *Chem. Soc. Rev.* **2006**, *35*, 1150−1161.
(12) Schoer, J. K.; Crooks, R. M. *Langmuir* **1997**, *13*, 2323−2332.
(13) Wadu-Mesthrige, K.; Amro, N. A.; Garno, J. C.; Xu, S.; Liu, G.-Y. *Biophys. J.* **2001**, *80*, 1891−1899.
(14) Liu, M.; Amro, N. A.; Chow, C. S.; Liu, G.-Y. *Nano Lett.* **2002**, *2*, 863−867.
(15) Liu, G.-Y.; Amro, N. A. *Proc. Natl. Acad. Sci. U.S.A.* **2002**, *99*, 5165−5170.
(16) Kaholek, M.; Lee, W.-K.; LaMattina, B.; Caster, K. C.; Zauscher, S. Nano *Lett.* **2004**, *4*, 373−376.
(17) Amro, N. A. Xu, S.; Liu, G.-Y. *Langmuir* **2000**, *16*, 3006−3009.
(18) Zhou, D.; Wang, X.; Birch, L.; Rayment, T.; Abell, C. *Langmuir* **2003**, *19*, 10557−10562.
(19) Brewer, N. J. Ph.D. Thesis, University of Manchester Institute of Science and Technology, 2002.
(20) Foster, T. T. Ph.D. Thesis, University of Manchester Institute of Science and Technology, 2004.
(21) Maoz, R.; Frydman, E.; Cohen, S. R.; Sagiv, J. *Adv. Mater.* **2000**, *12*, 424−429.
(22) Maoz, R.; Frydman, E.; Cohen, S. R.; Sagiv, J. *Adv. Mater.* **2000**, *12*, 725−731.
(23) Textor, M.; Ruiz, L.; Hofer, R.; Rossi, A.; Feldman, K.; Hahner, G.; Spencer, N. D. *Langmuir* **2000**, *16*, 3257−3271.
(24) Tosatti, S.; Michel, R.; Textor, M.; Spencer, N. D. *Langmuir* **2002**, *18*, 3537−3548.
(25) Zwahlen, M.; Tosatti, S.; Textor, M.; Hahner, G. *Langmuir* **2002**, *18*, 3957−3962.
(26) Spori, D. M.; Venkataraman, N. V.; Tosatti, S.; Durmaz, F.; Spencer, N. D.; Zurcher, S. *Langmuir* **2007**, *23*, 8053−8060.
(27) Gao, W.; Dickinson, L.; Grozinger, C.; Morin, F. G.; Reven, L. *Langmuir* **1996**, *12*, 6429.
(28) Ramsier, R. D.; Henrikson, P. N.; Gent, A. N. *Surf. Sci.* **1988**, *203*, 72.
(29) Dubois, L. H.; Nuzzo, R. G. *Ann. Rev. Phys. Chem.* **1992**, *43*, 437.
(30) Cao, G.; Hong, H.-G.; Mallouk, T. E. *Acc. Chem. Res.* **1992**, *25*, 420.
(31) Byrd, H.; Whipps, S.; Pike, J. K.; Ma, J.; Nagler, S. E.; Talham, D. R. *J. Am. Chem. Soc.* **1994**, *116*, 295.
(32) Foster, T. T.; Alexander, M. R.; Leggett, G. J.; McAlpine, E. *Langmuir* **2006**, *22*, 9254.
(33) Afrossman, S. M.; MacDonald, S. M. *Langmuir* 1996, *12*, 2090−2095.

NL072181+